A Chance Constrained Information-Gap Decision Model for Multi-Period Microgrid Planning

Xiaoyu Cao, *Student Member, IEEE*, Jianxue Wang, *Member, IEEE*, and Bo Zeng, *Member, IEEE*

***Abstract*—This paper presents a chance constrained information gap decision model for multi-period microgrid expansion planning (MMEP) considering two categories of uncertainties, namely random and non-random uncertainties. The main task of MMEP is to determine the optimal sizing, type selection, and installation time of distributed energy resources (DER) in microgrid. In the proposed formulation, information gap decision theory (IGDT) is applied to hedge against the non-random uncertainties of long-term demand growth. Then, chance constraints are imposed in the operational stage to address the random uncertainties of hourly renewable energy generation and load variation. The objective of chance constrained information gap decision model is to maximize the robustness level of DER investment meanwhile satisfying a set of operational constraints with a high probability. The integration of IGDT and chance constrained program, however, makes it very challenging to compute. To address this challenge, we propose and implement a strengthened bilinear Benders decomposition method. Finally, the effectiveness of proposed planning model is verified through the numerical studies on both the simple and practical complex microgrid. Also, our new computational method demonstrates a superior solution capacity and scalability. Compared to directly using a professional mixed integer programming solver, it could reduce the computational time by orders of magnitude.**

***Index Terms*—Microgrid, multi-period expansion planning, information gap decision theory, chance constrained program, bilinear Benders decomposition.**

NOMENCLATURE

Index

d	Index of day.
h	Index of hour.
k	Index of DER.
t	Index of year.

Parameters

η_k	Charge/discharge efficiency of ESS k.
ω	Minimum installation ratio of DFGs.
$\tau(t)$	Present value factor in tth year
$\tilde{\psi}^t$	Nominal estimate of demand capacity in tth year
A_k^{tdh}	Available power capacity of RES k at hth hour in dth day of tth year
c_k	Unit fuel cost of DFG k
$C_{\text{ann}}^{\max}$	Upper limit of annual investment cost
D	Number of typical days in a year
$E_k^{\max}$	Unit storage capacity of ESS k
EC_k	Unit energy cost of ESS k.
H	Number of hours in a day.
IC_k	Unit investment cost of DER k (except for ESS).
OC_k^t	Fixed operation and maintenance cost rate of DER k
OR^{tdh}	Short-term reserve requirement for microgrid at hth hour in dth day of tth year
$P_k^{\max}$	Unit power capacity of DER k
p_{L}^{tdh}	Load variation factor at hth hour in dth day of tth year
PC_k	Unit power cost of ESS k
q_{v}	Penalty cost for load curtailment
r	Discount rate
R^t	Long-term reserve requirement for microgrid in tth year
RD_k	Ramp down rate of DFG k
RU_k	Ramp up rate of DFG k
T	Number of years
$X_k^{\max}$	Upper limit of annual installation of DER k

Variables

α_{L}	Horizon of load uncertainty
E_k^{tdh}	Stored energy of ESS k at hth hour in dth day of tth year
P_k^{tdh}	Power generation of RES and DG k at hth hour in dth day of tth year
P_{lc}^{tdh}	Load curtailment at hth hour in dth day of tth year
$P_{k,\text{ch}}^{tdh}$	Charge power of ESS k at hth hour in dth day of tth year
$P_{k,\text{dis}}^{tdh}$	Discharge power of ESS k at hth hour in dth day of tth year
X_k^t	Number of installed DER k in tth year

Manuscript received January 27, 2017; revised May 17, 2017 and July 26, 2017; accepted August 24, 2017. Date of publication August 31, 2017; date of current version April 17, 2018.This work was supported in part by the Natural Science Basic Research Plan in Shaanxi Province of China under Grant 2016JM5072, in part by the National Natural Science Foundation of China under Grant 51777155, in part by the U.S. National Science Foundation under Grant CMMI-1635472, and in part by the Department of Energy grant DE-OE0000842. Paper no. TPWRS-00120-2017. *(Corresponding author: Jianxue Wang.)*

X. Cao and J. Wang are with the School of Electrical Engineering, Xi'an Jiaotong University, Xi'an 710049, China (e-mail: cxykeven2013@stu.xjtu.edu.cn; jxwang@mail.xjtu.edu.cn).

B. Zeng is with the Department of Industrial Engineering and the Department of Electrical and Computer Engineering, University of Pittsburgh, Pittsburgh, PA 15106 USA (e-mail: bzeng@pitt.edu).

Digital Object Identifier 10.1109/TPWRS.2017.2747625

I. INTRODUCTION

MICROGRID has been considered as a viable solution for the integration and management of distributed energy resources (DER) [1], which typically include renewable energy sources (RES), energy storage system (ESS), dispatchable fuel-generators (DFG), etc. The primary goal of multi-period microgrid expansion planning (MMEP) is to determine the op-

timal sizing, type selection, and installation time of DERs. The multi-period investment strategy is considered as an effective way to reduce the budget level of microgrid planning [2], which would benefit the development and commercialization of microgrid technology in the long run.

However, it is very challenging to manage the uncertainties in microgrid expansion planning. First, the intermittency of renewable energy generation increases the randomness of nodal power injection [3]. Second, the rapid development of renewable energy industry brings non-trivial uncertainties into the long-term investment of power sources [4]. At last, it is difficult to predict the load in a microgrid exactly due to the lack of historical data as well as the disaggregated environment of distributed generation system [5]. Either underestimating or overrating the impact of uncertainties in planning decisions could possibly jeopardize the power-supply reliability and cost-benefit of a microgrid.

In order to develop an advanced uncertainty management scheme, it is necessary to classify the uncertainties for MMEP problem. Here, we adopt the classical categorization for uncertain factors used in [6]–[9]:

1) Random uncertainties follow the specified probability distributions, which are high-frequency and repeatable in the short period. The hourly variation of load and RES generation is a typical example in this category.
2) Non-random uncertainties occur in lower frequency and larger time scale, which are difficult to accurately fit into any distribution due to data insufficiency. The uncertainties in demand growth fall into this category.

Probabilistic optimization methods, e.g. stochastic program (SP) and chance constrained program (CCP), are popular tools to manage the random uncertainties in microgrid planning. The main idea of SP is to employ a finite set of scenarios to represent the possible realizations of random variables. Ref [10] utilized SP to optimize the one-dispose investment for ESS in microgrid, where the random scenarios of RES generation were involved. Similar method was adopted in [2] for the capacity expansion planning of wind turbines (WT) and ESS in a stand-alone microgrid. Typically, an SP model considers every scenario in the scenario pool, which may lead to a costly solution that is less practical. Unlike SP, the key idea of CCP is to derive a solution that performs well in a subset of scenarios with a probabilistic guarantee, e.g., a solution works well in 90% random situations. Hence, CCP is a decision-making scheme providing a trade-off between cost and performance. Typical applications of CCP in microgrid planning can be found in [11]–[13]. Ref [11] presented a simulation based multi-objective CCP model to derive the single-stage planning solution of a stand-alone microgrid. Such simulation-based framework was also adopted in [12] to solve a chance constrained planning problem that addressed the siting and sizing of DERs in a distribution network. Ref [13] applied CCP to design a hybrid renewable energy system considering the random generation of WT and photovoltaic arrays (PV). We also note that a couple of other probabilistic methods have also been adopted to handle the randomness in microgrid planning, e.g., Markovian sizing approach [14], sample average approximation method [15], and conditional value-at-risk (CVaR) [16], which have different trade-offs between modeling advantages and computational requirements. The common feature of those methods is to make use of the uncertainty information contained in rich data. However, they are less applicable when data is unavailable or inaccurate.

The microgrid planning under non-random uncertainties, whose distributions are unknown, has been investigated using uncertainty set based approaches, e.g., robust optimization (RO) and information gap decision theory (IGDT). They only need uncertainty sets rather than probability distributions and make planning decisions under the worst scenarios within those sets. Ref [17] proposed and computed a two-stage RO based microgrid planning model. Ref [3] studied microgrid planning using an RO scheme to consider the uncertainties embedded in long-term load forecast, volatility of RES generation, and unintentional islanding. Different from RO, which requires a fixed uncertainty set with explicit boundaries, IGDT seeks to maximize the horizon of the uncertainty set over which the target system performance can be guaranteed [18]–[20]. Hence, for the situation where the target system performance is clear (e.g., the desired cost in the operational stage), IGDT helps the planner to identify a planning solution (subject to that cost restriction) with a maximized capacity to handle future uncertainties. In this regard, IGDT needs even less information about uncertainty structure [21], which makes it applicable for the problems under unstructured uncertainties. Certainly, when the uncertainty set can be defined well and the objective is economic-driven, RO could be more appropriate. Existing applications of IGDT include expansion planning of generation system [22] and transmission network [23].

Based on the literatures, we note that the choice of planning strategy largely depends on the type of uncertain factors. It becomes much more complicated when the distribution information is partially available, e.g., there is a mixture of random and non-random uncertainties. Such case, which usually happens in practical planning problems, demands for an integrated optimization framework to manage both types of uncertainties. Hence, a chance constrained information-gap decision (IGD) model is proposed in this paper. Our microgrid planning formulation considers multi-period investment scheme and detailed operational modeling to capture the uncertainties under multiple timescales, i.e., 1) the non-random uncertainty of yearly demand growth; 2) the random uncertainties of hourly RES generation and load variation. We follow the study presented in [2], [11], [13] to derive a planning solution for a stand-alone microgrid. Compared to a grid-supported system, the stand-alone microgrid is typically more vulnerable to uncertain factors, which hence requires us to use advanced optimization methods to incorporate those factors in system design. We note that the proposed model can also be extended to study a grid-connected microgrid by including additional decision variables and operational constraints concerning the power exchange between the microgrid and the utility grid. Also, considering a situation with a close proximity and a short electrical connection between load and DERs in microgrids [24], we do not include the network transmission and associated reactive power or power factor issue in our model.

Next, we summarize the main contributions of the presented research:

1) We construct the MMEP model under an integrated optimization framework of IGDT and CCP. In the derived framework, IGDT is applied to maximize the robustness level against non-random uncertainties through multi-period investment strategy, while the chance constraints are imposed in the operational stage to provide a flexible scheme to balance the random uncertainties and operational cost.
2) To compute this integrated model, a strengthened customization of bilinear Benders decomposition method [25] is developed with some non-trivial changes to adapt it for further reducing the computational burden from the complicated combinatorial structure.
3) We implement a series of comparative numerical tests on a simple test microgrid to examine the validity of the proposed planning method given the existence of both random and non-random uncertainties. Also, the scalability of our computational method is verified by a practical complex microgrid.

The remainder of this paper is organized as below. Section II provides the basic form of MMEP problem. Section III derives the mathematical formulation of chance constrained IGD model for microgrid planning. Section IV illustrates the solution approach of strengthened bilinear Benders decomposition. Section V shows the results of numerical tests. Finally, conclusions are drawn in Section VI.

II. Multi-Period Microgrid Expansion Planning

The basic form of MMEP problem contains a least-cost objective function and a set of constraints from investment and operational considerations, which restrict investment and operational decisions of alternative DERs. Three categories of DERs are considered, i.e., $\mathrm{DER} = \{\mathrm{RES}, \mathrm{DFG}, \mathrm{ESS}\}$. Our basic MMEP model, which characterizes the multi-period investment and long-term scheduling schemes, is formulated as:

$$\min \mathrm{TB} = \sum_{t=1}^{T} \tau(t)(C_{\mathrm{inv}}^{t} + C_{\mathrm{opr}}^{t}) \tag{1}$$

$$C_{\mathrm{inv}}^{t} = \sum_{k\in\{\mathrm{RES},\mathrm{DFG}\}} IC_k P_k^{\max}(X_k^t - X_k^{t-1}) + \sum_{k\in\mathrm{ESS}} (PC_k P_k^{\max} + EC_k E_k^{\max})(X_k^t - X_k^{t-1}) \ \forall t \tag{2}$$

$$C_{\mathrm{opr}}^{t} = \sum_{k\in\mathrm{DER}} OC_k^t P_k^{\max}(X_k^t - X_k^{t-1}) + \sum_{d=1}^{D}\sum_{h=1}^{H} \frac{365}{D}\left(\sum_{k\in\mathrm{DFG}} c_k P_k^{tdh} + q_{\mathrm{v}} P_{\mathrm{lc}}^{tdh}\right) \quad \forall t \tag{3}$$

$$\text{s.t.} \quad C_{\mathrm{inv}}^{t} \le C_{\mathrm{ann}}^{\max} \quad \forall t \tag{4}$$

$$X_k^{t-1} \le X_k^t \quad \forall k, \forall t \tag{5}$$

$$0 \le X_k^t \le X_k^{\max} \quad \forall k, \forall t \tag{6}$$

$$\sum_{k\in\mathrm{DER}} P_k^{\max} X_k^t \ge \psi^t + R^t \quad \forall t \tag{7}$$

$$\sum_{k\in\mathrm{DFG}} P_k^{\max} X_k^t \ge \omega\psi^t \quad \forall t \tag{8}$$

$$\sum_{k\in\{\mathrm{RES},\mathrm{DFG}\}} P_k^{tdh} + \sum_{k\in\mathrm{ESS}} (P_{k,\mathrm{dis}}^{tdh} - P_{k,\mathrm{ch}}^{tdh}) \ge \psi^t p_{\mathrm{L}}^{tdh} - P_{\mathrm{lc}}^{tdh} \quad \forall t, \forall d, \forall h \tag{9}$$

$$0 \le P_k^{tdh} \le X_k^t A_k^{tdh} \quad \forall k \in \mathrm{RES}, \forall t, \forall d, \forall h \tag{10}$$

$$X_k^t P_k^{\min} \le P_k^{tdh} \le X_k^t P_k^{\max} \quad \forall k \in \mathrm{DFG}, \forall t, \forall d, \forall h \tag{11}$$

$$-RD_k \le P_k^{tdh} - P_k^{tdh-1} \le RU_k \ \forall k \in \mathrm{DFG}, \forall t, \forall d, \forall h \tag{12}$$

$$\sum_{k\in\mathrm{DFG}} (X_k^t P_k^{\max} - P_k^{tdh}) \ge OR^{tdh} \quad \forall t, \forall d, \forall h \tag{13}$$

$$0 \le P_{k,\mathrm{ch}}^{tdh} \le X_k^t P_k^{\max} \quad \forall k \in \mathrm{ESS}, \forall t, \forall d, \forall h \tag{14}$$

$$0 \le P_{k,\mathrm{dis}}^{tdh} \le X_k^t P_k^{\max} \quad \forall k \in \mathrm{ESS}, \forall t, \forall d, \forall h \tag{15}$$

$$X_k^t E_k^{\min} \le E_k^{tdh} \le X_k^t E_k^{\max} \quad \forall k \in \mathrm{ESS}, \forall t, \forall d, \forall h \tag{16}$$

$$E_k^{tdh} = \sum_{i=1}^{h} (\eta_k P_{k,\mathrm{ch}}^{tdi} - P_{k,\mathrm{dis}}^{tdi}/\eta_k) \ \forall k \in \mathrm{ESS}, \forall t, \forall d, \forall h \tag{17}$$

$$E_k^{td0} = E_k^{tdH} \quad \forall k \in \mathrm{ESS}, \forall t, \forall d \tag{18}$$

$$X_k^t \in \mathbb{Z}_+ \quad \forall k, \forall t \tag{19}$$

$$P_k^{tdh}, P_{k,\mathrm{ch}}^{tdh}, P_{k,\mathrm{dis}}^{tdh}, E_k^{tdh}, P_{\mathrm{lc}}^{tdh} \in \mathbb{R}_+ \quad \forall k, \forall t, \forall d, \forall h \tag{20}$$

In the above formulation, the objective function (1) minimizes the total budget (TB) of microgrid over the planning horizon. It consists of the investment cost (C_{inv}^{t}) and operational cost (C_{opr}^{t}). In (2), the investment costs, which are proportional to the nominal capacity and installation number of DERs, are calculated on the yearly basis. In (3), the operational costs include fixed operation and maintenance (O&M) cost, fuel consumption cost, and load curtailment cost. The first term, O&M cost, is estimated as the fixed yearly rate of DERs' installation. The rest terms are calculated on the daily basis and then scaled to yearly values. The fuel cost of DFGs is quantified using the linear cost factor that synthesized from the fuel consumption rate and the generation efficiency [26] of each unit. The load curtailment cost is expressed as the product of load reduction and penalty factor. Overall, TB is evaluated as the net present value, where $\tau(t) = (1+r)^{-t}$ denotes the present value factor.

Constraints (4)–(8) are investment constraints. The annual investment cost is constrained by (4). Constraint (5) imposes the logic relationship of DERs' installation over consecutive years. The number of installed DERs in each year is constrained by (6). Constraint (7) keeps the annual installation of DERs larger than the summation of peak load and long-term reserve. Constraint (8) regulates the minimum installation of DFGs, which serve as the stable power sources in a stand-alone system. Constraints (9)–(18) are operational constraints. Constraint (9) ensures that

the hourly power supply can fully cover the load in microgrid. Note that load curtailment (P_{lc}^{tdh}) performs as a slack variable in (9), whose value can be naturally confined by imposing a large penalty factor (q_{v}). In (10), the generation of RESs is constrained by their available capacities, which are relevant to real-time resource conditions, e.g., wind speed and solar irradiation. The generic constraints of dispatchable generators are presented in (11)–(13). The allowable generation range and hourly ramping capability of DFGs are constrained by (11) and (12), respectively. Constraint (13) ensures that the short-term reserve provided by DFGs can satisfy the operational requirement of microgrid [27]. The operational states of ESS are constrained by (14)–(18) [2]. Since the operation of ESS is evaluated in independent days, their energy states in the first and last hours of each day should be kept the same. Finally, the decision variables in investment and operational problems are defined in (19) and (20), respectively.

As mentioned, MMEP problem is associated with a variety of random and non-random uncertainties. In (9), we assume that the load can be decomposed into demand capacity (ψ^t) and load variation factor (p_{L}^{tdh}) [28]. The primary source of non-random uncertainties results from the forecast error of demand capacity growth, which can be described using the envelope bound model [21]:

$$\Gamma(\alpha_{\mathrm{L}}, \tilde{\psi}) = \left\{ \psi : |(\psi_t - \tilde{\psi}_t)/\tilde{\psi}_t| \leq \alpha_{\mathrm{L}} \ \mid \alpha_{\mathrm{L}} \geq 0, \forall t \right\} \quad (21)$$

with $\tilde{\psi}_t$ being the forecasted value of demand capacity in each year. α_{L} is the horizon of demand growth uncertainty, which defines the information gap between the forecasted demand levels and the actual values. Generally, for a fixed $\tilde{\psi}_t$, a greater α_{L}, i.e., a stronger risk-tolerance capability, requires a more capacitated and costly planning solution for the microgrid.

On the other hand, the load variation factor (p_{L}^{tdh}) in each hour can be considered as the high-frequency component of load, which is classified as random uncertainties. Other types of random variables include the hourly power generation of RESs (A_{res}^{tdh}), which refers to WT and PV in this paper. Detailed probabilistic models of these random factors can be found in [29], [30].

Next, to better reflect the impact of random and non-random uncertainties, we extend our basic deterministic model to a chance constrained information-gap decision model.

III. Formulation of Chance Constrained Information-Gap Decision Model

A. Deterministic MMEP Model

In the following, we first provide a matrix representation of the deterministic model assuming the nominal estimates of uncertain variables to avoid a cumbersome exposition.

$$\min \quad \Lambda(x, y, \tilde{\psi}) = c^T x + d^T y \quad (22)$$

$$\text{s.t.} \quad Ax \geq b \quad (23)$$

$$Hx - W\tilde{\psi} \geq h \quad (24)$$

$$Sy - L\tilde{\psi} \geq 0 \quad (25)$$

$$-Fx + Ty \geq 0 \quad (26)$$

$$Gy \geq g \quad (27)$$

$$x \in \mathbb{Z}_+, y \in \mathbb{R}_+ \quad (28)$$

In (22), the budget function of deterministic model is denoted by $\Lambda(x, y, \tilde{\psi})$, where x and y are the vectors of investment and operational variables, respectively. The variables x are constrained by (23), corresponding to constraints (4)–(6). Constraints (24) and (25) correlate x and y with the forecasted value of demand growth ($\tilde{\psi}$), corresponding to constraints (7)–(8) and (9) respectively. Constraint (26) builds the relationship between x and y, corresponding to constraints (10)–(16). Rest constraints concerning y are represented by (27).

Remark 1: For an easy description, some equality constraints in (4)–(18) are represented as inequalities in (23)–(27). Note that there is no loss of generality as one equality (e.g. $a = b$) can always be equivalently replaced by a pair of inequalities (e.g. $a \leq b$ and $a \geq b$).

B. Information-Gap Decision Model for Microgrid Planning

In this paper, information gap decision theory (IGDT) is applied to address the non-random uncertainties in MMEP. The main idea of IGDT is to find a solution with maximized horizon of uncertainty as well as acceptable system performance [21]. To hedge against the load uncertainty, the information-gap decision (IGD) model can be written as:

$$\max_{x,y} \quad \alpha_{\mathrm{L}} \quad (29)$$

$$\text{s.t.} \quad \bar{\Lambda} \leq (1+\sigma)\Lambda_0 \quad (30)$$

$$Hx - W\psi \geq h \quad (31)$$

$$Sy - L\psi \geq 0 \quad (32)$$

$$\text{Eqs. } (23), (26) - (28) \quad (33)$$

$$\bar{\Lambda} = \max_{\psi \in \Gamma(\alpha_{\mathrm{L}}, \tilde{\psi})} \{\Lambda(x, y, \psi)\} \quad (34)$$

Note that the IGD model is actually a bi-level optimization problem. The upper level in (29) aims to maximize the horizon of load uncertainty meanwhile satisfying constraints (30)–(33). Constraint (30) is named as the 'budget level limit', which keeps the total budget ($\bar{\Lambda}$) lower than a specified level $(1+\sigma)\Lambda_0$. In this expression, Λ_0 represents the desired budget level under the expected situation, while σ is the deviation factor that specifies the acceptable degree of budget excess. Constraints (31) and (32) associate the decision variables with demand growth uncertainty (ψ). In (34), the lower level determines the robust performance of MMEP, i.e., the required budget level, to hedge against any possible variation of ψ in the set of $\Gamma(\alpha_{\mathrm{L}}, \tilde{\psi})$.

By analyzing our basic deterministic model in Section II, it can be easily seen that the largest budget requirement occurs when load achieves its upper bound, which is $\psi = (1+\alpha_{\mathrm{L}})\tilde{\psi}$. Hence, the bi-level structure can be simplified by replacing (30)–(32) and (34) with following (35)–(37).

$$c^T x + d^T y \leq (1+\sigma)\Lambda_0 \quad (35)$$

$$Hx-(1+\alpha_{\mathrm{L}})W\tilde{\psi}\geq h \tag{36}$$

$$Sy-(1+\alpha_{\mathrm{L}})L\tilde{\psi}\geq 0 \tag{37}$$

Eqs. (29), (33), (35)–(37) make up the single-level MIP formulation of IGD model. As shown in the objective function (29), which is to maximize the horizon of load uncertainty, a standard IGD model is good at dealing with a single uncertainty factor. When multiple uncertain factors are involved, it becomes less attractive. One idea is to extend it within a multi-objective optimization scheme (e.g., [31]). Another idea, as demonstrated in Section III-C, is to use scenarios to consider random factors whose probability distributions are available. Certainly, such an integrated model is large-scale, and generally demands for a customized powerful computational method, which will be addressed in Section IV. We also note that parameter σ is to control the deviation from the desired budget level. It is set according to the user's insights and preference. Nevertheless, if it is inappropriately selected, the IGD model could be overly conservative. This difficulty can also be addressed by the following chance constrained model where the budget level limit can be relaxed for some extreme situations.

C. Chance Constrained Information-Gap Decision Model

We mention that IGD model does not consider the random factors, which, however, is very critical in the operational stage. So, to further consider the random uncertainties (ξ) in MMEP, we replace the coefficient matrices in (26) and (37) by a set of stochastic matrices, corresponding to a set of stochastic scenarios. Definitely, the budget level limit (30) and power supply constraints (37) can be imposed for every realization of ξ. However, this requirement could be too restrictive, and practically they are allowed to be violated under some extreme situations. Hence, we impose a chance constraint to ensure that (30) and (37) are satisfied with a predefined probability. By doing so, the essential part of chance constrained IGD model can be written as:

$$\mathbb{P}\left\{\begin{array}{l} c^{T}x+d^{T}y(\xi)\leq(1+\sigma)\Lambda_{0} \\ Sy(\xi)-(1+\alpha_{\mathrm{L}})L(\xi)\tilde{\psi}\geq 0 \end{array}\right\}\geq 1-\varepsilon \tag{38}$$

$$-F(\xi)x+Ty(\xi)\geq 0 \tag{39}$$

$$Gy(\xi)\geq g \tag{40}$$

Note that the chance constrained IGD model takes a step forward by incorporating random ξ in the operational stage, whose joint probability space is defined in set $\Omega\subseteq\mathbb{R}$. Constraint (38) requires that the budget level limit and power supply constraints should be satisfied with a probability no less than $1-\varepsilon$, where ε denotes the risk tolerance level. In (38) and (39), random matrices $L(\xi)$ and $F(\xi)$ are associated with the distributions of load variation and RES generation, respectively.

To solve this type of problem, one popular approach is to convert the chance constrained model into a deterministic equivalence if the $1-\varepsilon$ quantile of the underlying distribution can be analytically represented. However, this method is not applicable for the joint probabilistic constraints, which demand for multi-variate integration. Indeed, our chance constraint (38) combines a set of constraints and several random variables, which makes it infeasible to derive a closed-form expression of the $1-\varepsilon$ quantile. Thus, we adopt a sampling strategy to represent the randomness by a finite set of discrete scenarios $\Omega=\{\xi_1,\xi_2,...,\xi_N\}$, and formulate a novel bilinear model of chance constrained program [25]. The bilinear formulation of chance constrained IGD model can be written as:

$$\max \quad \alpha_{\mathrm{L}} \tag{41}$$

$$\text{s.t.} \quad \text{Eqs. (23), (36)} \tag{42}$$

$$\left[c^{T}x+d^{T}y_{n}-(1+\sigma)\Lambda_{0}\right](1-z_{n})\leq 0 \quad \forall n \tag{43}$$

$$\left[Sy_{n}-(1+\alpha_{\mathrm{L}})L_{n}\tilde{\psi}\right](1-z_{n})\geq 0 \quad \forall n \tag{44}$$

$$-F_{n}x+Ty_{n}\geq 0 \quad \forall n \tag{45}$$

$$Gy_{n}\geq g \quad \forall n \tag{46}$$

$$\sum_{n=1}^{N}\pi_{n}z_{n}\leq\varepsilon \tag{47}$$

$$\alpha_{\mathrm{L}}\geq 0, x\in\mathbb{Z}_{+} \tag{48}$$

$$y_{n}\in\mathbb{R}_{+}, z_{n}\in\{0,1\}, n=1,...,N \tag{49}$$

In the aforementioned model, α_{L} and x are first-stage variables, while y_n denotes second-stage operational (i.e., recourse) variables. The budget level limit is decomposed into a set of constraints. All the budget level constraints share the same first-stage cost $c^{T}x$, but with separated recourse cost $d^{T}y_{n}$ defined in each scenario. The first-stage problem is only related to non-random uncertainties, which is subject to constraints (42). The second-stage recourse problem is associated with both random and non-random uncertainties, which is subject to constraints (43)–(47).

Chance constraint (38) is replaced by the bilinear structure in (43) and (44). The binary variable z_n is employed to indicate the full requirements of scenario n is imposed or not. When $z_n=1$, (43) and (44) can be ignored, i.e., those constraints are deactivated, and only (45) and (46) are necessary. Otherwise, the complete constraints of scenario n, i.e., (43)–(46), must be satisfied. The total probability of scenarios that are partially satisfied is restricted by (47), where π_n denotes the realization probability of scenario n.

Remark 2: Note that if $z_n=1$, which means that constraints in (43) and (44) will be ignored. For the remaining constraints associated with scenario n, i.e., (45) and (46), we mention that it is always feasible to define a feasible y_n for any given x. The reason behind is that (45) and (46), which represent (10)–(18) in the basic deterministic model, define the feasible set for every single operation variable that is never empty. Thus, we can easily generate y_n satisfying those constraints for any fixed x. Moreover, given that the objective function in (41) does not depend on y_n, we can conclude that (45) and (46) alone do not impact the choice of the first-stage decision variables (α_{L},x). Note that such observation allows us to simply focus on the impact of (43) and (44) by making decisions on the selection of scenario n.

Overall, the CC-IGD based microgrid planning model in (41)–(49) gives a full consideration to the random and non-random uncertainties defined in Section II. On one hand, the multi-period investment decisions are made to maximize the risk-tolerance towards long-term uncertainty of demand growth. On the other hand, the hourly operational decisions are made under each scenario to hedge against the random uncertainties of renewable energy generation and load variation. Next, we present an effective computational method to solve this sophisticated model.

IV. Solution Approach

The mixed-integer nonlinear formulation presented in (41)–(49) for MMEP could be very difficult to compute, even for the case with a small number of scenarios to capture randomness. To address such computational challenge, we follow the idea presented in [25] to develop a strengthened bilinear Benders decomposition algorithm to solve the proposed planning problem. As a decomposition method, our algorithm involves a master problem and two subproblems. Before proceed to concrete algorithm steps, we describe subproblems in the follows.

Our first subproblem, which is referred to the economic dispatch subproblem (EDS) for a single scenario, is to minimize the recourse cost $d^T y_n$ subject to other constraints in the second stage, i.e., (44)–(46), for a given first stage solution, denoted by $(\hat{\alpha}_{\mathrm{L}}, \hat{x})$. Mathematically, it is

$$\mathbf{SP_1}: \ \hat{\Phi}_n = \min \ d^T y_n \tag{50}$$

$$\text{s.t.} \quad S y_n \geq (1+\hat{\alpha}_{\mathrm{L}}) L_n \tilde{\psi} : \mu_n \tag{51}$$

$$T y_n \geq F_n \hat{x} : \lambda_n \tag{52}$$

$$G y_n \geq g : \gamma_n \tag{53}$$

$$y_n, \mu_n, \lambda_n, \gamma_n \in \mathbb{R}_+ \tag{54}$$

where $\mu_n, \lambda_n, \gamma_n$ are dual variables of constraints (51)–(53), respectively. As mentioned, the aforementioned subproblem is defined for every single scenario.

Note that EDS is always feasible due to the load reduction variables (P_{lc}^{tdh}). According to the strategy in [25], we just need to supply a Benders optimality cut (OC) in the following bilinear form to the master problem.

$$\left[\hat{\Phi}_n + \hat{\mu}_n^T L_n(\alpha_{\mathrm{L}} - \hat{\alpha}_{\mathrm{L}}) + \hat{\lambda}_n^T F_n(x - \hat{x})\right](1 - z_n) \leq \Phi_n \tag{55}$$

where variable Φ_n is to represent EDS cost in the second stage and z_n is the binary indicator variable defined in (41)–(49).

Remark 3: (i) Unlike the traditional Bender decomposition method, OC is modulated by the binary indicator variable z_n. When $z_n = 1$, (55) reduces to a trivial constraint $\Phi_n \geq 0$, which means OC is deactivated. Otherwise, it is enforced in the master problem.

(ii) As mentioned earlier, when $z_n = 1$, only (45) and (46) are presented for scenario n. As they do not affect either the feasibility or the optimality of $(\hat{\alpha}_{\mathrm{L}}, \hat{x})$, we are not concerned by those constraints, except for their impact in $\mathbf{SP_1}$.

Another subproblem is designed to verify the feasibility of the first stage solution $(\hat{\alpha}_{\mathrm{L}}, \hat{x})$ to the original formulation in (41)–(49). Let t_n be the nth auxiliary variable. We have

$$\mathbf{SP_2}: \ \Delta = \min \sum_{n=1}^{N} t_n \tag{56}$$

$$\text{s.t.} \quad t_n \geq [c^T \hat{x} + \hat{\Phi}_n - (1+\sigma)\Lambda_0](1 - z_n) \ \forall n \tag{57}$$

$$\sum_{n=1}^{N} \pi_n z_n \leq \varepsilon \tag{58}$$

$$t_n \geq 0, z_n \in \{0,1\}, \ n = 1, 2, ..., N. \tag{59}$$

Remark 4: We can easily see that once $\Delta = 0$, $(\hat{\alpha}_{\mathrm{L}}, \hat{x})$ is a feasible solution of chance constrained IGD model. This property is actually critical to our Benders decomposition algorithm development. As we will show next, if an optimal solution of the master problem leads to zero optimal value in $\mathbf{SP_2}$, it is also optimal to the chance constrained IGD model.

In the following, we define the master problem (**IGDMP**) based on the strategy provided in [25]. Let $U_{n,i}(\alpha_{\mathrm{L}}, x) = \hat{\Phi}_{n,i} + \hat{\mu}_{n,i}^T L_n(\alpha_{\mathrm{L}} - \hat{\alpha}_{\mathrm{L},i}) + \hat{\lambda}_{n,i}^T F_n(x - \hat{x}_i)$, where i is the counter of iteration.

$$\max \quad \alpha_{\mathrm{L}} \tag{60}$$

$$\text{s.t.} \quad Ax \geq b \tag{61}$$

$$Hx - (1+\alpha_{\mathrm{L}}) W \tilde{\psi} \geq h \tag{62}$$

$$c^T x + \Phi_n - (1+\sigma)\Lambda_0 \leq 0 \quad \forall n \tag{63}$$

$$(1 - z_n) U_{n,i}(\alpha_{\mathrm{L}}, x) \leq \Phi_n \ i = 1, ..., j-1, \forall n \tag{64}$$

$$\sum_{n=1}^{N} \pi_n z_n \leq \varepsilon \tag{65}$$

$$\alpha_{\mathrm{L}} \geq 0, x \in \mathbb{Z}_+ \tag{66}$$

$$z_n \in \{0,1\}, \Phi_n \in \mathbb{R}_+, n = 1, ..., N \tag{67}$$

Similar to the conventional Benders decomposition method, OC in (64), in a bilinear form, will be generated from $\mathbf{SP_1}$ for every scenario and then supplied to this master problem in every iteration.

Remark 5: (i) The bilinear structure in (64) can be easily linearized by using McCormick linearization method [32]. For example, consider the bilinear term $x_k z_n (= \tilde{x}_k)$, where x_k is the k-th component variable of x. It can be replaced by the linear constraints and variables in (68), given that $\bar{x}_k$ is an upper bound of x_k. As a result, the master problem is converted into an MIP problem that can readily be computed by any professional MIP solver.

$$\tilde{x}_k \leq \bar{x}_k z_n, \ \tilde{x}_k \leq x_k, \ \tilde{x}_k \geq x_k - \bar{x}_k(1 - z_n), \ \tilde{x}_k \geq 0 \tag{68}$$

(ii) Nevertheless, the linearization in (68) will introduce a large amount of new variables and constraints, which makes it computational cumbersome to solve the **IGDMP**. To address this shortcoming, we adopt an equivalent replacement for the

Algorithm 1: Strengthened Bilinear Benders Decomposition.

Initialization:

Set $j = 0$ and $\Delta_j = +\infty$;$OC_{n,j} = \emptyset$;

Iteration:

1: **while** $\Delta_j > 0$ **do**
2: $\quad \mathbf{IGDMP}_j \leftarrow \mathbf{IGDMP}_{j-1} \bigcup_{n=1}^{N} \{OC_{n,j}\}$;
3: $\quad$ Compute master problem $\mathbf{IGDMP}_j$;
4: $\quad$ **if** $\mathbf{IGDMP}_j$ is infeasible **then**
5: $\quad\quad$ terminate and *report the infeasibility*;
6: $\quad$ **else**
7: $\quad\quad$ Get solution $(\hat{\alpha}_{\mathrm{L}}^j, \hat{x}^j, \hat{z}^j)$;
8: $\quad$ **end if**
9: $\quad j \leftarrow j + 1$;
10: $\quad$ **for** $n = 1$ to N **do**
11: $\quad\quad$ Compute $\mathbf{SP}_1$ to get $(\hat{\Phi}_{n,j}, \hat{\mu}_{n,j}, \hat{\lambda}_{n,j})$;
12: $\quad\quad$ Generate optimality cut $OC_{n,j}$;
13: $\quad$ **end for**
14: $\quad$ Compute $\mathbf{SP}_2$ to get Δ_j;
15: **end while**
16: **output:** Report $(\hat{\alpha}_{\mathrm{L}}^j, \hat{x}^j)$.

bilinear formulation in (63) and (64):

$$c^T x + \Phi_n(1 - z_n) - (1 + \sigma)\Lambda_0 \leq 0 \quad \forall n \tag{69}$$

$$U_{n,i}(\alpha_{\mathrm{L}}, x) \leq \Phi_n \quad i = 1, ..., j-1, \forall n \tag{70}$$

The equivalence can be argued by considering (63)–(64) and (69)–(70) in both $z_n = 0$ and $z_n = 1$ situations. When $z_n = 0$, (63) and (64) reduce to (69) and (70). And when $z_n = 1$, $\Phi_n \geq 0$ and hence Φ_n can be simply set to 0 in (63), which indicates that an optimal (α_L, x) to $\mathbf{IGDMP}$ is not affected by $U_{n,i}(\alpha_{\mathrm{L}}, x)$ or Φ_n. Note that the same effect is also achieved in (69) due to $\Phi_n(1 - z_n) = 0$.

We mention that linearization of (69) requires a much less number of newly-added variables and constraints than that from linearization of (64). Hence, the modified $\mathbf{IGDMP}$ with (69)–(70) could be solved in a more efficient way. In the rest of this paper, we denote Benders decomposition with this improvement as **strengthened bilinear Benders Decomposition** while the one with (63) and (64) as the original one.

(iii) Note that the master problem is a relaxation to the chance constrained IGD model in (41)–(49), which will be strengthened by iteratively adding (64). Consider its optimal solution $(\hat{\alpha}_{\mathrm{L}}, \hat{x})$. If the corresponding $\mathbf{SP}_2$ returns zero, which verifies that it is feasible to (41)–(49), we can conclude that it is also optimal to (41)–(49).

With the well-defined subproblems and the master problem, the complete steps of our method is outlined in Algorithm 1.

Remark 6: The algorithm of Strengthened Bilinear Benders Decomposition terminates with an optimal solution to (41)–(49) or report infeasibility in a finite number of iterations.

Note that whenever $\mathbf{SP}_2$ has a strictly positive optimal value, i.e., the latest optimal solution to the master problem is not feasible to the original CC-IGD model, a set of new extreme points (i.e., their corresponding OC cuts) will be included into the master problem $\mathbf{IGDMP}$. It must differ from those generated in previous iterations. Otherwise, the new master problem is same as that in the previous iteration. However, given the connection between (63)–(64) and $\mathbf{SP}_2$, we can conclude that both master problems (because they are identical) are infeasible, which, according to **Algorithm** 1's description, terminates the whole algorithm.

Note also that the feasible set of dual problem to $\mathbf{SP}_1$ has a finite number of extreme points, which is the basis of Benders OC cuts, for every scenario. Hence, we conclude that the algorithm will either produce an optimal solution or terminate with infeasibility in a finite number of iterations.

V. Numerical Results

In this section, the proposed planning model and computation approach are firstly demonstrated in a simple microgrid through a series of comparative numerical tests. Then, we further test our method on a practical microgrid with complex structure to prove its scalability. All the algorithm development and computations, including our bilinear Benders decomposition, are made by CPLEX in MATLAB environment on a desktop computer with Intel Core i5-3470 3.20 GHZ processer.

A. Simple Microgrid

In this case, the proposed method is tested on a stand-alone microgrid with a simple structure. The candidate DERs include wind turbines (WT), photovoltaic panels (PV), diesel engine (DE), micro turbine (MT), and battery packs (ES), whose major parameters are listed in Table I. The planning horizon is 10 years with 5 separated periods. The discount rate is set to 4%. The initial demand capacity is 450 kW and its growth rate is forecasted to be 8% per year. The penalty cost for load curtailment is specified as 5 $/ kWh. Four typical days are selected from each year to represent the seasonal and diurnal patterns of RES generation and load variation. According to the historical data in [33], 2000 scenarios are produced using Monte Carlo simulation. Overall, each scenario contains three time-series for wind, solar, and load respectively, each of which has totally 960 sampling points.

First, we will exhibit the basic planning results. To make a compromise between the computational accuracy and efficiency, scenario reduction is performed to extract 80 representative scenarios for problem solving. Next, the risk-averse capability of proposed CC-IGD model will be compared with deterministic and IGD-based MMEP models through performance evaluation, where the entire scenario set is included. Moreover, sensitivity analysis will be performed to investigate the impact of key control parameters, i.e., deviation factor σ and risk tolerance level ε, on planning results. Last but not the least, the computational feasibility of strengthened bilinear Benders decomposition method (SBD) will be tested.

1) Basic Planning Results: To better illustrate the planning results of CC-IGD, we choose the deterministic MMEP model (DT) in Section III-A and the IGD model (IGD) in Section III-B as benchmarks. The parameters are set as deviation factor

TABLE I
SIMPLE MICROGRID: PARAMETERS OF CANDIDATE DERS

Distributed Generators							
Label	Type	Power Cap. (kW)	Min Output (kW)	Capital Cost ($/kW)	O&M Cost ($/kW/yr)	Fuel Cost ($/kWh)	Num Limit
WT	Wind Turbine	120	0	900	0	/	3
PV	Photovolatic	80	0	1200	0	/	3
DE	Diesel Engine	60	10	300	175.2	0.105	2
MT	Micro Turbine	80	10	450	262.8	0.089	2

Energy Storage Devices								
Label	Type	Power Cap. (kW)	Energy Cap. (kWh)	Power Cost ($/kW)	Energy Cost ($/kWh)	O&M Cost ($/kW/yr)	Efficiency	Num Limit
ES1	Battery Pack 1	90	150	270	150	23.4	0.95	4
ES2	Battery Pack 2	100	200	200	180	35	0.85	4

TABLE II
SIMPLE MICROGRID: PLANNING RESULTS

Period	DER Type	#CC-IGD#	DT	IGD
I Year 1–2	RES	WT = 360 kW PV = 240 kW	WT = 360 kW PV = 240 kW	WT = 360 kW PV = 240 kW
	DFG	DE = 120 kW MT = 160 kW	DE = 120 kW MT = 160 kW	DE = 120 kW MT = 160 kW
	BES	ES1 = 600 kWh ES2 = 200 kWh	ES1 = 600 kWh ES2 = 400 kWh	ES1 = 600 kWh ES2 = 200 kWh
II Year 3–4	RES	WT = 240 kW PV = 240 kW	WT = 360 kW PV = 240 kW	WT = 360 kW PV = 240 kW
	DFG	DE = 60 kW MT = 160 kW	MT = 160 kW	MT = 160 kW
	BES	ES1 = 450 kWh ES2 = 600 kWh	ES1 = 600 kWh ES2 = 800 kWh	ES1 = 600 kWh ES2 = 800 kWh
III Year 5–6	RES	PV = 240 kW	WT = 120 kW PV = 160 kW	WT = 240 kW PV = 240 kW
	DFG	MT = 160 kW	0	MT = 80 kW
	BES	/	ES2 = 400 kWh	ES1 = 150 kWh ES2 = 800 kWh
IV Year 7–8	RES	WT = 120 kW	WT = 120 kW	WT = 120 kW
	DFG	DE = 80 kW	DE = 120 kW	MT = 80 kW
	BES	ES1 = 150 kWh	ES1 = 150 kWh	/
V Year 9–10	DFG	/	/	DE = 60 kW

$\sigma = 0.4$, risk tolerance level $\varepsilon = 0.1$. Under given conditions, the objective value of DT is minimized as $\Lambda_0 = \$5,425,087$, which determines the desired budget level for IGD and CC-IGD computation. Set the budget limit as $1.4 \times \$5,425,087$, the robustness level ($\alpha_{\mathrm{L}}$) maximized by IGD and CC-IGD are 0.1742 and 0.0857, respectively. CC-IGD derives lower α_{L} due to its extra consideration for random factors. Table II presents the solutions of different MMEP models. We regard DT solution as the basic scheme, while the solutions of IGD and CC-IGD as the reinforcement. To prepare for the unexpected demand growth, IGD makes comprehensive reinforcement by installing 200 kW more RES, 100 kW more DFGs, and 200 kWh more ESS. Different from the IGD solution, the reinforcement made by CC-IGD seems to be more selective. First, CC-IGD brings forward the installation of 60 kW DE from Period V to Period II. Then, the WT installation is reduced from 600 kW to 240 kW at Period II & III. Instead, CC-IGD adds the capacity of MT from 80 kW to 160 kW at Period III. All these changes could reduce the random risks brought by RES output and load variation while retaining system's robustness against non-random uncertainties.

2) Performance Evaluation of Chance Constrained IGD Model: The risk-averse capability of CC-IGD solution is further examined through post performance evaluation. The performance metric for planning schemes is defined as the Expected Project Budget (EPB), which can be calculated as:

$$EPB = c^T x + \frac{1}{NS} \sum_{n=1}^{NS} d^T y_n \tag{71}$$

where variables x and y_n are defined as in Section III. NS denotes the number of scenarios, which is set to 2000 in this case.

The performance metrics of CC-IGD solution are computed and compared with those of DT and IGD solutions under different robustness levels (α_{L}), as shown in Table III. The maximum load capacity during the planning horizon is intuitively presented in Column "Peak". When $\alpha_{\mathrm{L}} = 0$ (Peak = 900 kW), the evaluation results of different models are close to each other. When $\alpha_{\mathrm{L}} = 0.1$ (Peak = 990 kW), the EPB of CC-IGD solution is \$7,065,800, which is below the budget level limit, i.e.,

TABLE III
SIMPLE MICROGRID: RESULTS OF PERFORMANCE EVALUATION

α_L	Peak	Expected Project Budget		
		DT	IGD	CC-IGD
0.00	900 kW	$5,928,600	$6,043,800	$5,780,000
0.10	990 kW	$7,918,000	$7,261,600	$7,065,800
0.20	1080 kW	$10,904,000	$9,018,400	$8,647,100

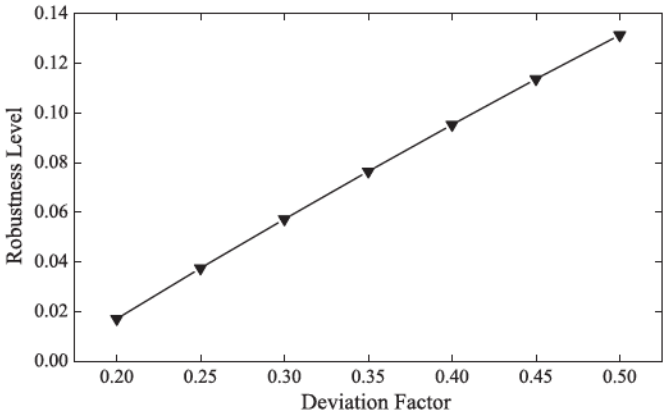

(a)

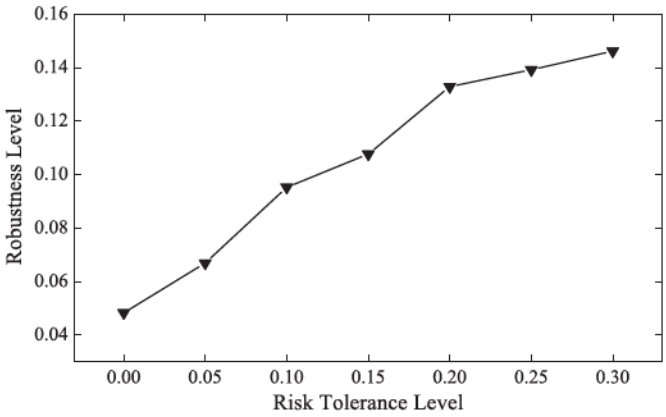

(b)

Fig. 1. Sensitivity Analysis of Model Parameters. (a) Deviation Factor. (b) Risk Tolerance Level.

$\$1.4 \times 5,425,087 = 7,595,122$. In contrast, the EPB of DT solution exceeds the budget limit by $322,878 due to the costly penalty for load curtailment. When $\alpha_L = 0.2$ (Peak = 1,080 kW), both DT and CC-IGD solutions violate the budget level limit. That is because $\alpha_L = 0.2$ is far beyond the maximum robustness level that can be tolerated by CC-IGD solution, i.e., 0.0857. However, the CC-IGD solution costs 20.70% less than the DT. These observations prove the validity of the proposed CC-IGD model. Moreover, CC-IGD shows better performance than the IGD model in every instance, which reduces the budget expectation by more than $195,800. Hence, CC-IGD shows a superiority over DT and IGD under the co-existence of random and non-random uncertainties.

TABLE IV
SIMPLE MICROGRID: SOLUTION PERFORMANCE UNDER DIFFERENT SCENARIO NUMBERS

NS	OBJ	#SBD#			CPX		OBD		
		itr	min	gap	min	gap	itr	min	gap
20	0.1014	9	17.5		399.4		7	22.1	
40	0.0953	10	43.6		T	N/A	7	163.1	
60	0.0863	11	133.6		T	N/A	/	T	429.1%
80	0.0857	8	138.5		T	N/A	/	T	671.2%

TABLE V
SIMPLE MICROGRID: SOLUTION PERFORMANCE UNDER DIFFERENT PERIOD NUMBERS

NP	OBJ	#SBD#			CPX		OBD		
		itr	min	gap	min	gap	itr	min	gap
3	0.0055	5	12		T	5.06%	5	37.7	
5	0.0953	10	43.6		T	N/A	7	163.1	
10	0.2295	10	146		T	N/A	/	T	378.9%

3) Sensitivity Analysis of Key Control Parameters: To analyze the impact of key control parameters, we solve the proposed planning model under different values of deviation factor (σ) and risk tolerance level (ε). Fig. 1(a) exhibits the varying trend of robustness level (α_L) of CC-IGD solution with respect to σ, which is the acceptable budget excess with respect to the desired budget from deterministic model. Fixing $\varepsilon = 0.10$ while changing σ from 0.20 to 0.50 with a step of 0.05, the robustness level improves from 0.0171 to 0.1314, which represents an increased immunity against uncertainties. This observation confirms an intuition that a larger σ leads to a more capable planning solution to handle the long-term demand growth uncertainty.

Similarly, Fig. 1(b) presents the trend of robustness level via changing ε. As implied by CCP, a larger ε leads a softer budget limit, i.e., more violations of budget limit are allowed over stochastic scenarios. Equivalently, more operational scenarios can be ignored in our MMEP planning model, which allows us to allocate more resources to maximize our capacity on handling the long-term demand growth uncertainty. Such insight is verified in our numerical study. Fixing $\sigma = 0.4$ while changing ε from 0.00 to 0.30 with a step of 0.05, the robustness level grows from 0.0483 to 0.1462. Clearly, we can adjust ε in CC-IGD model to achieve a balanced microgrid investment plan under both the long-term and operational uncertainties.

4) Computational Test of Strengthened Bilinear Benders Decomposition Method: The computational feasibility of SBD is verified by comparing to the original Benders decomposition (OBD) form, which adopts (63) and (64) in its master problem, and the direct use of CPLEX (CPX). Again, McCormick linearization method is applied to convert (41)–(49) into mixed-integer linear formulation so that it can be directly solved by CPLEX. The solution time is counted by minutes, which has a limit up to 600 mins. If any problem is terminated due to the time limit, its solution time will be labeled as "T". The remaining gap or "N/A" (in case the gap cannot be reported) will be marked beside it.

TABLE VI
COMPLEX MICROGRID: PARAMETERS OF CANDIDATE DERS

Distributed Generators							
Label	Type	Power Cap. (kW)	Min Output (kW)	Capital Cost ($/ kW)	O&M Cost ($/ kW/yr)	Fuel Cost ($/ kWh)	Num Limit
WT1	Wind Turbine	240	0	900	0	/	4
WT2	Wind Turbine	360	0	750	0	/	4
PV1	Photovolatic	100	0	1150	0	/	4
PV2	Photovolatic	180	0	1000	0	/	4
DE1	Diesel Engine	120	20	280	131.4	0.095	2
DE2	Diesel Engine	150	30	250	131.4	0.099	2
DE3	Diesel Engine	200	40	230	131.4	0.109	2
MT1	Micro Turbine	160	15	420	236.5	0.086	2
MT2	Micro Turbine	200	20	380	236.5	0.091	2
FC1	Fuel Cell	80	0	620	289.1	0.137	2
FC2	Fuel Cell	100	0	590	289.1	0.156	2

Energy Storage Devices								
Label	Type	Power Cap. (kW)	Energy Cap. (kWh)	Power Cost ($/ kW)	Energy Cost ($/ kWh)	O&M Cost ($/ kW/yr)	Efficiency	Num Limit
ES1	Battery Pack 1	100	200	340	220	20	0.95	6
ES2	Battery Pack 2	150	200	280	220	20	0.9	6
ES3	Battery Pack 3	200	300	250	170	30	0.85	6
ES4	Battery Pack 4	300	300	200	170	30	0.8	6

Table IV presents the test results under different numbers of scenario (NS). The objective level, iteration number, solution time, and remaining gap are recorded in columns "α_{L}", "itr", "min", and "gap", respectively. The result indicates that bilinear BD method, even in its original form, performs better than the direct use of CPLEX. Only when $NS = 20$ can all the algorithms converge to an optimal solution. SBD derives the same result as CPX but performs an order of magnitude faster, saving the solution time by 95.62%. For the rest instances when scenario size gets larger, CPX either fails to derive any feasible solutions or cannot solve the linear programming relaxation within the time limit, which leads to no gap information available.

Also, the strengthened bilinear BD significantly outperforms its original counterpart (OBD). When $NS = 20, 40$, both methods succeed in solving the problem, but SBD is observed to be much faster. When $NS = 60$ and 80, only SBD can derive the optimal solution within the time limit. Compared to OBD, SBD might need more iterations to converge but achieves a tremendous time-saving in each iteration. Therefore, our modification in the bilinear Benders decomposition method has clearly improved its computational efficiency.

Furthermore, the comparison between SBD and benchmark algorithms under different numbers of period (NP) are shown in Table V. It indicates that the robustness level of solution evidently improves with the increase of NP, which, however, makes it more challenging to solve the problem. In all instances, only SBD and OBD can converge to an optimal solution. When $NP = 3$, CPX is terminated at the gap of 5.06% due to the time limit, which leads to a sub-optimal solution. Nevertheless, when $NP = 5$, CPX fails to report a feasible solution. In contrast, our SBD demonstrates a remarkable solution capacity, which not only solves the problem successfully, but also saves the solution time by 73.27%, compared to OBD. Note that when $NP = 10$, only SBD can successfully solve the problem, while OBD can only report a low quality solution with a very large gap. Hence, comparing to CPX or OBD, SBD performs faster by orders of magnitude.

B. Complex Microgrid

The proposed planning method is further applied to optimize the investment portfolio of a practical microgrid with complex structure. Detailed parameters of candidate DERs, including 4 types of RES, 7 types of DFGs, and 4 types of ESS, are listed in Table VI. In this case, 4 planning periods are considered over 12 years. The initial load capacity is 1.25MW and the forecasted demand growth is 10% per year. The budget level limit is specified as $1.3 \times \$15,624,525.12$ while the risk tolerance level is set to 0.10. Table VII presents the planning result of complex microgrid. We observe that the DERs with lower capital cost (WT2, PV2, and ES4) or lower fuel cost (DE1 and MT1) are installed with a high priority, which ensures the cost-effectiveness of solution. The robustness level of CC-IGD solution is maximized as $\alpha_{\mathrm{L}} = 0.1052$ by properly sizing the DERs' combination. On

TABLE VII
COMPLEX MICROGRID: PLANNING RESULTS

Period	DER Type	Planning Scheme
I Year 1–3	RES	WT1 = 480 kW WT2 = 1440 kW PV1 = 400 kW PV2 = 720 kW
	DFG	DE1 = 240 kW DE2 = 300 kW MT1 = 320 kW MT2 = 400 kW
	BES	ES3 = 1800 kWh ES4 = 1800 kWh
II Year 4–6	RES	WT2 = 1440 kW PV2 = 720 kW
	DFG	DE1 = 240 kW DE2 = 150 kW MT1 = 320 kW
	BES	ES3 = 1800 kWh ES4 = 1800 kWh
III Year 7–9	RES	WT2 = 1080 kW PV2 = 180 kW
	DFG	DE1 = 240 kW MT1 = 320 kW
	BES	ES4 = 1200 kWh
IV Year 10–12	RES	WT2 = 360 kW
	DFG	DE1 = 120 kW MT1 = 320 kW

TABLE VIII
COMPLEX MICROGRID: SOLUTION PERFORMANCE OF DIFFERENT METHODS

NS	OBJ	#SBD#			CPX		OBD		
		itr	min	gap	min	gap	itr	min	gap
10	0.1101	18	115.5		T	9.84%	15	613.0	
40	0.0916	16	646.6		T	N/A	/	T	315.2%
80	0.1052	14	1844.0		T	N/A	/	T	689.3%

one hand, each kilowatt of RES is equipped with 1.23 kWh storage device to deal with resource uncertainties. On the other hand, over 2900 kW DFGs (30% of total generation capacity) are installed over 12 years to ensure the power-supply reliability under demand growth uncertainty. Hence, the derived planning scheme gives a full consideration to the complex uncertain environment of microgrid.

Also, the computational test of proposed solution approach is performed on a complex microgrid under different numbers of scenarios. The solution time limit is set to 2000 mins, which is moderate for a practical planning problem. As indicated by the test results in Table VIII, this practical system with 10 scenarios is extremely challenging for CPX to compute. This instance, however, can be well addressed by both bilinear BD methods. Moreover, with the number of scenarios growing, SBD demonstrates its superiority over OBD by successfully solving all the instances (including an intractable 80-scenario instance) using at most 1844 mins. On the contrary, OBD fails to close the optimality gap for instances with more than 10 scenarios. Together with our observations made on the computational study using the simple microgrid, we can conclude that the customized SBD has a superior scalable capacity to handle MMEP with multiple planning periods and stochastic scenarios.

VI. CONCLUSION

In this paper, a chance constrained IGD model is proposed to manage the uncertainties in MMEP problem. This model is formulated under an integrated framework of IGDT and chance constrained program, which aims to maximize the robustness level of DER investment meanwhile satisfying a set of operational constraints with a high probability. Furthermore, a strengthened bilinear Benders decomposition algorithm is developed to solve the problem. Two sets of experiments are presented to verify the proposed planning method. We observe that our chance constrained IGD model is competent to address the risks and challenges from both random and non-random uncertainties within a multi-period planning scheme. Also, our strengthened bilinear Benders Decomposition method demonstrates a strong solution capacity and scalability to compute the chance constrained IGD model for practical microgrids. Therefore, it enables us to make informative planning decision in a more efficient way.

REFERENCES

[1] N. Hatziargyriou, H. Asano, R. Iravani, and C. Marnay, "Microgrids," *IEEE Power Energy Mag.*, vol. 5, no. 4, pp. 78–94, Jul./Aug. 2007.
[2] E. Hajipour, M. Bozorg, and M. Fotuhi-Firuzabad, "Stochastic capacity expansion planning of remote microgrids with wind farms and energy storage," *IEEE Trans. Sustain. Energy*, vol. 6, no. 2, pp. 491–498, Apr. 2015.
[3] A. Khodaei, S. Bahramirad, and M. Shahidehpour, "Microgrid planning under uncertainty," *IEEE Trans. Power Syst.*, vol. 30, no. 5, pp. 2417–2425, Sep. 2015.
[4] C. Jeon and J. Shin, "Long-term renewable energy technology valuation using system dynamics and monte carlo simulation: Photovoltaic technology case," *Energy*, vol. 66, no. 4, pp. 447–457, 2014.
[5] L. Hernandez, C. Baladron, J. M. Aguiar, and B. Carro, "A survey on electric power demand forecasting: Future trends in smart grids, microgrids and smart buildings," *IEEE Commun. Survey Tuts.*, vol. 16, no. 3, pp. 1460–1495, Third Quart. 2014.
[6] W. J. Burke, H. M. Merrill, F. C. Schweppe, B. E. Lovell, M. F. McCoy, and S. A. Monohon, "Trade off methods in system planning," *IEEE Trans. Power Syst.*, vol. 3, no. 3, pp. 1284–1290, Aug. 1988.
[7] M. O. Buygi, G. Balzer, H. M. Shanechi, and M. Shahidehpour, "Market-based transmission expansion planning," *Energy Power Eng.*, vol. 4, no. 4, pp. 387–391, 2004.
[8] M. O. Buygi, H. M. Shanechi, G. Balzer, and M. Shahidehpour, "Network planning in unbundled power systems," *IEEE Trans. Power Syst.*, vol. 21, no. 3, pp. 1379–1387, Aug. 2006.
[9] P. Maghouli, S. H. Hosseini, M. O. Buygi, and M. Shahidehpour, "A scenario-based multi-objective model for multi-stage transmission expansion planning," *IEEE Trans. Power Syst.*, vol. 26, no. 1, pp. 470–478, Feb. 2011.
[10] S. Bahramirad, W. Reder, and A. Khodaei, "Reliability-constrained optimal sizing of energy storage system in a microgrid," *IEEE Trans. Smart Grid*, vol. 3, no. 4, pp. 2056–2062, Dec. 2012.
[11] L. Guo, W. Liu, B. Jiao, B. Hong, and C. Wang, "Multi-objective stochastic optimal planning method for stand-alone microgrid system," *IET Gener. Transm. Distrib.*, vol. 8, no. 7, pp. 1263–1273, 2014.
[12] Z. Liu, F. Wen, and G. Ledwich, "Optimal siting and sizing of distributed generators in distribution systems considering uncertainties," *IEEE Trans. Power Del.*, vol. 26, no. 4, pp. 2541–2551, Oct. 2011.
[13] A. Kamjoo, A. Maheri, and G. A. Putrus, "Chance constrained programming using non-gaussian joint distribution function in design of standalone hybrid renewable energy systems," *Energy*, vol. 66, no. 4, pp. 677–688, 2014.
[14] J. Dong, F. Gao, X. Guan, Q. Zhai, and J. Wu, "Storage-reserve sizing with qualified reliability for connected high renewable penetration micro-grid," *IEEE Trans. Sustain. Energy*, vol. 7, no. 2, pp. 732–743, Apr. 2016.
[15] M. Sharafi and T. Y. Elmekkawy, "Stochastic optimization of hybrid renewable energy systems using sampling average method," *Renew. Sustain. Energy Rev.*, vol. 52, no. 1, pp. 16–25, 2015.

[16] R. Mena, M. Hennebel, Y. F. Li, C. Ruiz, and E. Zio, "A risk-based simulation and multi-objective optimization framework for the integration of distributed renewable generation and storage," *Renew. Sustain. Energy Rev.*, vol. 37, no. 3, pp. 778–793, 2014.
[17] A. Billionnet, M. C. Costa, and P. L. Poirion, "Robust optimal sizing of a hybrid energy stand-alone system," *Eur. J. Oper. Res.*, vol. 254, no. 2, pp. 565–575, 2016.
[18] Y. Ben-Haim, *Info-Gap Decision Theory*. 2nd ed. San Diego, CA, USA: Academic, 2006.
[19] B. Mohammadi-Ivatloo, H. Zareipour, N. Amjady, and M. Ehsan, "Application of information-gap decision theory to risk-constrained self-scheduling of gencos," *IEEE Trans. Power Syst.*, vol. 28, no. 2, pp. 1093–1102, May 2013.
[20] J. Aghaei *et al.*, "Optimal robust unit commitment of CHP plants in electricity markets using information gap decision theory," *IEEE Trans. Smart Grid*, vol. 8, no. 5, pp. 2296–2304, Sep. 2016.
[21] M. Kazemi, B. Mohammadi-Ivatloo, and M. Ehsan, "Risk-constrained strategic bidding of gencos considering demand response," *IEEE Trans. Power Syst.*, vol. 30, no. 1, pp. 376–384, Jan. 2015.
[22] M. Shivaie and M. T. Ameli, "A stochastic framework for multi-stage generation expansion planning under environmental and techno-economic constraints," *Electr. Power Compon. Syst.*, vol. 44, no. 17, pp. 1917–1934, 2016.
[23] M. Taherkhani and S. H. Hosseini, "IGDT-based multi-stage transmission expansion planning model incorporating optimal wind farm integration," *Int. Trans. Elect. Energy Syst.*, vol. 25, no. 10, pp. 2340–2358, 2014.
[24] A. Khodaei, "Microgrid optimal scheduling with multi-period islanding constraints," *IEEE Trans. Power Syst.*, vol. 29, no. 3, pp. 1383–1392, May 2014.
[25] B. Zeng, Y. An, and L. Kuznia, "Chance constrained mixed integer program: Bilinear and linear formulations, and Benders decomposition," *Tech. Rep.*, 2014.
[26] M. H. Moradi, M. Eskandari, and S. Mahdi Hosseinian, "Operational strategy optimization in an optimal sized smart microgrid," *IEEE Trans. Smart Grid*, vol. 6, no. 3, pp. 1087–1095, May 2015.
[27] B. Zhao, Y. Shi, X. Dong, W. Luan, and J. Bornemann, "Short-term operation scheduling in renewable-powered microgrids: A duality-based approach," *IEEE Trans. Sustain. Energy*, vol. 5, no. 1, pp. 209–217, Jan. 2014.
[28] M. Rahmani-Andebili, "Distributed generation placement planning modeling feeders failure rate and customers load type," *IEEE Trans. Ind. Electron.*, vol. 63, no. 3, pp. 1598–1606, Mar. 2016.
[29] R. Billinton and D. Huang, "Effects of load forecast uncertainty on bulk electric system reliability evaluation," *IEEE Trans. Power Syst.*, vol. 23, no. 2, pp. 418–425, May 2008.
[30] O. Ekren and B. Y. Ekren, "Size optimization of a PV/wind hybrid energy conversion system with battery storage using response surface methodology," *Appl. Energy*, vol. 85, no. 11, pp. 1086–1101, 2008.
[31] S. Dehghan, A. Kazemi, and N. Amjady, "Multi-objective robust transmission expansion planning using information-gap decision theory and augmented ε-constraint method," *IET Gener. Transm. Distrib.*, vol. 8, no. 5, pp. 828–840, 2013.
[32] G. P. Mccormick, "Computability of global solutions to factorable nonconvex programs: Part I-convex underestimating problems," *Math. Program.*, vol. 10, no. 1, pp. 147–175, 1976.
[33] X. Cao, J. Wang, and Z. Zhang, "Multi-objective optimization of preplanned microgrid islanding based on stochastic short-term simulation," *Int. Trans. Electr. Energy Syst.*, vol. 27, no. 1, pp. 1–16, 2017.

Xiaoyu Cao (S'17) received the B.S. degree in electrical engineering from the North China Electric Power University, Baoding, China, in 2013. He is currently working toward the Ph.D. degree in the School of Electrical Engineering, Xi'an Jiaotong University, Xi'an, China. His current research interests include microgrid planning and scheduling, and generation expansion planning.

Jianxue Wang (M'11) received the B.S., M.S., and Ph.D. degrees in electrical engineering from Xi'an Jiaotong University, Xi'an, China, in 1999, 2002, and 2006, respectively.

He is currently a Professor in the School of Electrical Engineering, Xi'an Jiaotong University. His current research interests include microgird planning and schdeuling, power system planning and scheduling, and electricity market.

Bo Zeng (M'11) received the Ph.D. degree in industrial engineering from Purdue University, West Lafayette, IN, USA. He currently is an Assistant Professor in the Department of Industrial Engineering and the Department of Electrical and Computer Engineering, University of Pittsburgh, Pittsburgh, PA, USA. His research interests include polyhedral study and algorithms for stochastic and robust mixed integer programs, coupled with applications in power and logistics systems. He is also a member of IISE and INFORMS.